

RESEARCH MEMORANDUM

TESTS OF AERODYNAMICALLY HEATED MULTIWEB WING STRUCTURES

IN A FREE JET AT MACH NUMBER 2

FOUR ALUMINUM-ALLOY MODELS OF 20-INCH CHORD AND SPAN
WITH 0.064-INCH-THICK SKIN, 0.025-INCH-THICK
RIBS AND WEBS, AND ZERO, ONE, TWO, OR

THREE CHORDWISE RIBS

By John R. Davidson, Richard Rosecrans, and Louis F. Vosteen

Langley Aeronautical Laboratory Langley Field, Va.

NATIONAL ADVISORY COMMITTEE FOR AERONAUTICS

WASHINGTON

May 8, 1958

NATIONAL ADVISORY COMMITTEE FOR AERONAUTICS

RESEARCH MEMORANDUM

TESTS OF AERODYNAMICALLY HEATED MULTIWEB WING STRUCTURES

IN A FREE JET AT MACH NUMBER 2

FOUR ALUMINUM-ALLOY MODELS OF 20-INCH CHORD AND SPAN
WITH 0.064-INCH-THICK SKIN, 0.025-INCH-THICK
RIBS AND WEBS, AND ZERO, ONE, TWO, OR

THREE CHORDWISE RIBS

By John R. Davidson, Richard Rosecrans, and Louis F. Vosteen

SUMMARY

Four multiweb wing models were tested at a Mach number of 2 in a free jet to investigate structural effects of aerodynamic heating and loading. The models had a 20-inch chord and span; a 5-percent-thick, circular-arc airfoil section; and three, two, one, or zero chordwise internal stiffening ribs. Each aluminum-alloy model had 0.064-inchthick skins, six 0.025-inch-thick spanwise webs, and 0.025-inch-thick tip bulkheads. The model with no internal ribs survived the first test at sea-level static pressure and a stagnation temperature of 930 F, but failed during the second test at a stagnation temperature of 5630 F. The other models survived all tests. Temperature and strain measurements were made on all models and the data were tabulated. Calculated stresses, determined from the temperature distribution on the model with one rib, are compared with the stresses determined from measured strains. The tests showed that the addition of a single rib maintained sufficient structural integrity to prevent flutter after loss of stiffness caused by thermal stress and reduced modulus of elasticity at elevated temperatures. Modes determined from laboratory vibration tests without heating show that the addition of only one rib nearly doubles the lowest frequency at which cross-sectional distortion occurs.

INTRODUCTION

This is part of a series of reports describing tests conducted by the Langley Structures Research Division to investigate the effects of combined aerodynamic heating and loading on built-up wing structures. Aerodynamic heating can reduce structural stiffness by lowering material moduli and inducing thermal stresses. Previous papers (refs. 1 to 4) describe the tests on the first seven models in this series. The first model (model MW-1) was of 40-inch chord and semispan and failed during a test in which the structure was subjected to aerodynamic heating. The second model (model MW-2) was essentially a half-scale version of model MW-l and had a 20-inch chord and semispan; this model also failed under similar test conditions. Both models were tested at a Mach number of 2 and a stagnation temperature near 500° F, and both developed flutter involving cross-sectional distortion which ended with the destruction of the models. Additional tests were made on models of the MW-2 design to obtain pressure data and to investigate the effect of angle of attack on the flutter mode. (See ref. 5.) Model MW-4 differed from model MW-2 only in the thickness of the tip bulkhead (0.025 inch thick for model MW-4 and 0.250 inch thick for model MW-2); model MW-4 failed in a manner similar to that of models MW-1 and MW-2. The remaining models (MW-3, MW-5, MW-6, and MW-7) survived similar tests.

The flutter and failure of models MW-2 and MW-4 indicated the need for additional initial stiffness to maintain sufficient structural resistance to flutter after aerodynamic heating had lowered the material moduli and thermal stresses had changed the stiffness of the built-up wing structure. (See refs. 6 and 7.) Consequently, the design of model MW-4 was modified by the addition of one, two, and three chordwise ribs in models designated MW-18, MW-17, and MW-16, respectively. In addition, another model identical to model MW-4, and designated MW-4-(2), was included in the test program covered in this report. These models were tested to measure model temperature and strain distributions, to confirm the previous conclusion that aerodynamic heating contributed to the failure of model MW-4, and to evaluate the effectiveness of chordwise ribs in preventing distortion of the cross section. The effects of chordwise ribs are discussed, and an attempt is made to correlate measured stresses with calculated stresses.

SYMBOLS

R radius, in.

T temperature, OF

T* normalized temperature, ${}^{\circ}F$; T_b * = $\frac{(T_t - T_o)_a}{(T_t - T_o)_b}(T - T_o)_b + T_o, a$

Tt stagnation temperature, OF

T_O initial temperature (model), ^OF

angle of attack, deg

Subscripts:

a test conditions experienced by model MW-18 during its first test

b test conditions or model temperatures under consideration

Stress, expressed in psi or ksi, is positive for tension and is negative for compression.

MODELS

Model Construction

Each semispan wing model had a 5-percent-thick, symmetrical, circular-arc airfoil section and was constructed from 2024-T3 aluminum alloy with a 20-inch chord and $24\frac{1}{8}$ -inch span of which $19\frac{7}{8}$ inches extended into the airstream. Internal construction consisted of six 0.025-inch-thick spanwise webs spaced $2\frac{1}{2}$ inches apart and three, two, one, or zero 0.025-inch-thick chordwise stiffening ribs with the number depending upon the particular model. All models had a 0.025-inch-thick tip bulkhead, 0.064-inch-thick skin, and solid leading and trailing edges. At the base of each model there were two 0.081-inch-thick doubler plates, a $2\frac{1}{2}$ -inch-thick root bulkhead, and two 1/2-inch-thick-steel clamping blocks for attaching the model to its supporting structure. Aluminum-alloy standard and blind rivets were used throughout. Sketches of each model showing individual construction details are found in figure 1. A photograph of the interior of model MW-16 prior to final assembly is shown in figure 2.

The model exteriors were painted with zinc chromate primer, upon which a black India ink grid was superimposed to help determine model

motions and deformations from motion-picture data. The effect of this paint on the heat transfer into the structure is small. (See ref. 4.)

Instrumentation

All models were instrumented with iron-constantan thermocouples with the beaded junctions peened into small holes drilled into the skins, webs, and ribs. Thermocouples mounted in the interior of the solid leading- or trailing-edge sections were first coated with cement and were then inserted into small holes drilled into these sections. Figure 3 shows the thermocouple locations for each model.

Figure 3 shows the locations where SR-4 type EBDF-7D temperature-compensated wire strain gages were attached to the models with thermosetting cement. These strain gages are compensated to read approximately zero strain when used on unstressed aluminum alloy at temperatures between 50° F and 250° F. The useful temperature range may be extended by first post-curing the gage cement to the maximum test temperature and then, after cooling to room temperature, calibrating the gage by slowly heating the model in an oven while measuring the indicated strain when load and thermal stresses are absent. The maximum model temperature expected during these tests was 450° F; inasmuch as heating the model to this temperature would change the aluminum-alloy properties, the gage cement was postcured to only 250° F and, therefore, gage accuracy was sacrificed to prevent changes in the material properties. The natural frequency of the galvanometers used to record strain data was about 100 cps; thus, these galvanometers were not suitable for measurement of high-frequency strain amplitudes.

The following list gives the estimated probable errors in individual measurements and the corresponding time constants. The time constant, which is considered independent of the probable error, is defined as the time at which the recorded value of a step-function input is 63 percent of that of the input; after three time constants, the response amounts to at least 95 percent of the input.

| Item | Probable error | Time constant, sec |
|------------------------|-----------------------|--------------------|
| Stagnation pressure | ±0.7 psi | 0.03 |
| Stagnation temperature | ±3° F | .12 |
| Model temperature | ±3° F | .03 |
| Model strain | ±150 microinches/inch | .02 |

Errors due to thermocouple installation have not been included but are believed to be small.

High-speed 16-millimeter motion pictures were taken of each test to record model behavior. The high-speed cameras had a frame rate of 600 to 1,600 frames per second. Monitor cameras running at 120 frames per second were used to augment the data supplied by the high-speed cameras. The cameras and oscillograms were correlated by using a common 1/10-second timing pulse.

APPARATUS AND PROCEDURE

Aerodynamic Test Facility

The tests were made in the preflight jet of the Langley Pilotless Aircraft Research Station at Wallops Island, Va. The preflight jet is a blowdown-type wind tunnel in which models are tested in a 27- by 27-inch free jet at the exit of a Mach number 1.99 supersonic nozzle. A description of the jet operation and characteristics may be found in reference 2.

Disturbances within the jet during the starting and shutdown periods cause violent model oscillations, and for some of these tests a retractable tip stabilizer was used to restrain the model until test conditions were reached. The stabilizer was activated at about 1 second after the start of the air flow, it released the model at 1.3 seconds, and it left the air-stream at about 1.7 seconds. Immediately preceding the shutdown period, at about 11 seconds, the stabilizer reentered the airstream and had fully gripped the model at about 12 seconds.

Laboratory Vibration Tests

Prior to the wind-tunnel tests, a vibration survey was made to find the natural modes and frequencies of each of the models. An electromagnetic shaker supplied energy to the model, and the response was detected by a phonograph-type pickup whose signal was fed into a cathode-ray oscilloscope. The frequencies were measured by a Stroboconn frequency meter.

Jet Tests

Figure 4 is a photograph of a typical model mounted on the jet test stand preparatory to an aerodynamic test. An aerodynamic fence surrounded the model base and protected the model instrumentation leads. The sharp leading edge of the fence was raised 1/8 inch above the bottom wall of the jet nozzle to scoop off a small boundary of air. The leading edge of the

model was located 2 inches from the nozzle-exit plane; this separation may have diminished as much as 1/4 inch during a high-stagnation-temperature test because the nozzle expanded toward the model.

All tests were conducted with the model oriented at zero angle of attack with respect to the jet center line.

Model MW-4-(2) was first tested at a stagnation temperature near ambient temperature (93° F) and then at a high stagnation temperature (563° F). Model MW-16 was first tested with the stagnation temperature near ambient temperature; the next three tests were made at elevated stagnation temperatures. The other two models were tested at the elevated temperatures only.

RESULTS AND DISCUSSION

Laboratory Vibration Tests

Vibration modes and frequencies for the models are indicated in table I. The node-line locations for individual model modes varied only slightly from the average locations sketched in this table. The addition of ribs changed mode C from one involving much chordwise distortion into a clear second bending mode, D. For model MW-4-(2), the lowest frequency at which chordwise distortion occurred was 268 cps. The addition of one rib to this design (to give model MW-18) increased the chordwise stiffness sufficiently to eliminate chordwise deflection below 465 cps, as is evident from the mode-pattern change between modes C and D. In all cases, whenever a single rib was added to the basic configuration the model frequency was raised; adding a second rib increased all frequencies again; but the addition of a third rib was accompanied by a decrease in the frequencies for modes A, B, and D, which may indicate that the added mass had more influence than the incremental change in stiffness. The MW-16 design (three ribs) was the only configuration that exhibited a distinct second torsion mode; the other designs seem to have had insufficient ribs to develop this form of vibration. It appears from these room-temperature tests that two chordwise ribs may represent optimum stiffening for a wing of this design.

Jet Tests

Test conditions. - A summary of the averaged test conditions is given in table II, and typical variations of stagnation pressure and temperature with time are plotted in figures 5 and 6, respectively. Test conditions were deemed to exist whenever the stagnation pressure exceeded 100 psia, which was the period from approximately 2 to 11 seconds after air began to flow into the jet. Averaged test conditions were determined from the

area under the quantity plotted against time curves for the 9 seconds during which test conditions existed.

Model data. - Data from the model instrumentation are presented primarily in tabular form, with values given at the even seconds during a test. All data herein are referenced to zero test time which was taken to occur when the static pressure in the jet nozzle 1 inch from the nozzle exit first deviated from ambient pressure. This occurrence is approximately 1.8 seconds before test conditions are reached.

The severe characteristic starting and shutdown disturbances of the jet destroyed some model instrumentation and caused other instruments to be unreliable. There were other instrumentation failures which probably were initiated by the starting shock but in which the instrument finally failed from a combination of heat and random disturbances. A gap was left in the data in the tables whenever an instrument failed or became unreliable.

The temperature data are presented in table III, and the strain data are presented in table IV. The tabulated strain values are the measurements read directly from the records with no corrections for errors caused by model-temperature changes.

Model Behavior

The behavior of the models during each test is summarized in table V and is described in detail in the following discussion. In addition, a motion-picture film supplement has been prepared of the two tests on model MW-4-(2) and of the second test on model MW-18 and is available on loan. A request-card form will be found at the back of this paper on the page immediately preceding the abstract and index pages.

No attempt was made to evaluate the amplitude of the oscillations from the strain-gage records at any time because the inherent instrumentation attenuation would create large inaccuracies in such an analysis. The exact beginning and ending of most of the recorded and observed oscillations were usually difficult to determine; hence, the times listed in the descriptions of the tests are given only to a valid number of significant figures for each respective measurement.

Test 1 of model MW-4-(2).- During test 1, strain gages 10 and 11 showed that model MW-4-(2) vibrated at 65 cps between 1.5 seconds and 1.8 seconds with a very small amplitude; this was after the jet starting disturbances had ceased. This slight movement was not discernible in the high-speed motion pictures. At 8.7 seconds small-amplitude oscillations commenced; strain gage 1 indicated a vibratory frequency of 130 cps. The motion pictures show that the small amplitude increased monotonically

until 9.5 seconds when the vibration stopped. No further motion was observed until 10.7 seconds when a slight torsional mode developed; strain gages 10 and 11 indicated a frequency of 80 cps, which changed slowly to 70 cps by 11.85 seconds. At 11.8 seconds a definite 173-cps oscillation was indicated by strain gage 1; the motion pictures show that a small-amplitude torsional vibration started at 10.7 seconds, reached a peak at 11.6 seconds, and then decayed to an unnoticeable movement at 12.3 seconds. At 12.5 seconds a torsional mode appeared and continued until the shutdown period, which started at 12.6 seconds.

Test 2 of model MW-4-(2).- After 1.0 second, the end of the starting disturbances of test 2 of model MW-4-(2), the motion pictures showed that a small vibrational mode at 72 cps was present, but it quickly disappeared in the pictures. However, strain gage 11 showed that a 72-cps vibration was present until failure. In the motion pictures the model remained stationary until 7.32 seconds, at which time a 238-cps flutter mode began; this mode ended with violent and complete destruction of the model. The wing apparently first vibrated with skin panel flutter, but the amplitudes were so small that exact modal identification was made difficult. By 7.42 seconds a mode involving chordwise distortion was identified. This motion became increasingly violent, and at 7.64 seconds the tip rib showed evidence of crippling failure at the right side of the model at web 4. (Webs were numbered from the leading edge to the trailing edge.) At the maximum displacement of this same point from the model neutral center line at 7.656 seconds, the rear portion of the tip rib was torn from the model. The next sign of progressive failure occurred at 7.672 seconds when a tear started at the leading edge near the base of the model. The tear reached the trailing edge at 7.677 seconds, and the remains of the model were carried downstream. Photographs of this failure sequence are shown in figure 7.

Test 1 of model MW-16. - During the period throughout which test conditions existed, no motion of model MW-16 during test 1 was visible in the motion pictures. Some intermittent small-amplitude oscillations, probably excited by random jet noise, were indicated by the strain-gage records. These frequencies were between 60 and 78 cps.

Test 2 of model MW-16. The strain-gage record of model MW-16 during test 2 showed some very small amplitude, random oscillations of intermittent duration at 275 to 286 cps from after the starting disturbances until the beginning of the shutdown period. At 10 seconds strain gage 9 showed a vibration of increasing amplitude with a frequency of 60 cps which may have actually started before 10 seconds, but the vibration was not large enough to cause a noticeable strain-gage signal. At 12 seconds this motion showed clearly in the motion pictures but died out after 13 seconds. At 13.3 seconds the shutdown disturbances began.

Test 3 of model MW-16. The model tip stabilizer was used during the starting and shutdown periods of test 3 of model MW-16. Although the motion pictures showed no visible movement, strain gage 19 indicated that a small-amplitude vibration, 258 to 266 cps, existed throughout the test.

Test 4 of model MW-16.- After the starting period of test 4, model MW-16 remained stable until 9 seconds when strain gage 9 indicated a small vibration at 60 cps which lasted until the shutdown disturbances began. For this test only one camera, operating at about 100 frames per second, was used; this motion could not be seen in these pictures.

Test 1 of model MW-17.- The strain-gage records of test 1 of model MW-17 indicate that some form of disturbance (probably random jet noise in the test house) caused the model to vibrate slightly at frequencies between 130 and 140 cps. After the tip stabilizer reentered the airstream preceding the shutdown period, the model developed a small torsional mode that was visible in the motion pictures. All strain gages indicated a frequency of 140 cps. The motion pictures indicated that the vibrations were intermittent from 10.9 seconds until the shutdown period.

Test 2 of model MW-17. - After the starting period of test 2 of model MW-17, there was no motion until 11 seconds when the tip stabilizer reentered the airstream. Then, a torsional mode developed at 140 cps and continued until the beginning of the shutdown disturbances.

Test 1 of model MW-18.- Model MW-18 remained stationary after the starting period of test 1. At 11 seconds when the tip stabilizer reentered the airstream, a torsional and bending mode of vibration commenced at a frequency of 145 cps which remained until the beginning of the shutdown period.

Test 2 of model MW-18. - Strain gages 11, 12, and 20 indicated some small vibration of model MW-18 during test 2 at a frequency of 70 cps between 5 seconds and the shutdown period. This vibration was not observed in the motion pictures. After the tip stabilizer had fully regripped the model, the pictures showed intermittent torsional vibration modes of first 124 cps and then, immediately preceding the shutdown disturbances, 70 cps; the 70-cps vibration was barely evidenced by strain gages 2 and 4. However, for the period between 11.6 seconds and 12.6 seconds, several frequencies could be obtained from the strain-gage traces; for instance, strain gage 13 showed a 275-cps frequency, strain gage 6 showed a 400-cps frequency, and strain gage 10 showed a 538-cps frequency. The small amplitudes and diversity of frequency suggest random excitation.

For times other than those during the starting, shutdown, and failure periods, all the noted vibrations were of small amplitude, probably resulting from the random noise and pressure disturbances in the vicinity

of the jet. Whenever the jet stagnation pressure was below 50 psi, which was from the start until about 1.2 seconds and also from about 13.4 seconds until complete shutdown of the jet, the model experienced violent buffeting; when the stagnation pressure was between 50 and 100 psi, the jet shock was passing over the model and creating random but much less violent disturbances. The presence of the tip stabilizer in the airstream prior to the shutdown period evidently disturbed the flow in a manner which excited the observed model torsional vibrations.

Temperatures

A typical temperature history of a skin and web is shown in figure 8 for a high-stagnation-temperature test. The temperature data from test to test were compared by normalizing the data with respect to the test conditions experienced by model MW-18 during test 1. The normalized temperature was determined from the formula

$$T_b^* = \frac{\left(T_t - T_0\right)_a}{\left(T_t - T_0\right)_b} \left(T - T_0\right)_b + T_0, a$$

where the subscript a refers to the test conditions which existed during the first test of model MW-18, and the subscript b refers to the test conditions or model temperatures for the particular model under consideration. The normalized temperatures plotted in figures 9 and 10 show that the agreement among the model-temperature data was very good. Figure 9 is a plot of the skin temperatures (midway between webs where the sink effect of the web is negligible) that existed at 6 seconds test time. In general, the skin temperatures decreased spanwise from the tip to the root and chordwise from the leading edge to the trailing edge. A temperature distribution was calculated by the method outlined in reference 4 using the Van Dreist method for calculating the heat-transfer coefficient; tunnelsurvey data were used to determine the adiabatic-wall temperature. It can be seen from figures 9(b), 9(c), and 9(d) that the spanwise distribution indicated in figure 9(a) is typical of each chord station. The spanwise temperature variation is attributed to the parabolic-like stagnationtemperature distribution that is a characteristic of the jet. The calculated line shown with the test data in figure 9(a) actually follows the measured variation in the jet stagnation temperature.

Figure 10 shows the difference in the normalized temperatures between the skin thermocouples and the web thermocouples for webs 3 and 4 at specific span stations. This difference generally increases spanwise because of the more rapid heating of the model at stations near the center of the jet stream. However, significant deviations from this general

distribution may be taken as a rough indication of the local joint conductivity. Figure 10 shows that, near the tip of model MW-18, the joint conductivity was considerably below average for web 3, but was above average for web 4.

Stresses

Experimental stresses. Inasmuch as the state of stress in the model skins was two-dimensional, stresses were determined from measured strains only at points where two perpendicular gages were mounted. In order to obtain the stresses at a given point, the chordwise and spanwise gages were considered as being superimposed upon each other at the location of the thermocouple placed between them. (See fig. 3(d).)

Several methods were tried in an attempt to account for temperature effects on the strain data obtained from the strain gages. Although no one method could be shown to lead to reliable and accurate strain data, especially in the temperature range above 250° F, inspection of the result indicated that the strain error could be as much as ±200 microinches per inch. This would cause a skin-stress error of about ±2,000 to 3,000 psi, which is of the same order of magnitude as the experimental stresses.

A survey of the strain data was made by using the measured values of strain at 6 seconds test time. These data indicate that at the model root the experimental chordwise strains were as much as twice the spanwise strains. The gages mounted on opposite skins in the center bay near the root indicate bending strains - counterclockwise strains (looking upstream) for models MW-17 and MW-18 and clockwise strains for model MW-4-(2); only one skin was instrumented at this point on model MW-16. The strain gages indicated tensile stresses in the ribs and webs (except in the tip rib in model MW-18 during the first test) for all the elevated-temperature tests. During the cold-temperature test on model MW-16, the rib strains were compressive; the conditions during this test were such that the model was cooled. Compared with the web strains, the rib strains were small, with a maximum rib strain (at 6 seconds) of 208 microinches per inch of tension on the middle rib of model MW-18 during the first test. This condition suggests that these ribs did not restrain the model skins as much in the chordwise direction as the webs did in the spanwise direction; this may be primarily due to the discontinuous nature of the ribs. The webs ran continuously over the span.

The strains measured on web 3 during the elevated-temperature tests on models MW-16, MW-17, and MW-18 were in the same range (822 to 953 microinches per inch of tension) at 6 seconds test time; whereas for the elevated-temperature test on model MW-4-(2), the strain at this point was 1,280 microinches per inch of tension.

At the time considered (6 seconds test time) the model skin temperatures were such that, because of imperfect strain-gage temperature compensation, the range of error in the indicated strains could be as much as ±100 microinches per inch.

Calculated stresses. The nonuniform temperature distribution over the models during high-stagnation-temperature tests gave rise to thermal stresses. Appendix E in reference 8 presents an approximate method for calculating these thermal stresses. This method, which does not take into account any influence on spanwise stresses caused by chordwise stresses, was used to calculate spanwise stresses at a cross section 3 inches from the tip of model MW-18, a section not influenced appreciably by chordwise ribs. At this section the general spanwise gradient was very small and was neglected. The experimental model temperatures (from test 1 of model MW-18) were used to determine the temperatures of the area elements shown in the idealized cross section in figure 11. Aerodynamic loads were neglected because it was assumed that, at zero angle of attack, only the drag force would appreciably add to the thermal stresses; preliminary calculations indicated that stresses due to drag load were less than 5 psi. End effects were also considered negligible at this section.

Figure 12 shows calculated skin stresses at the midchord and web stresses at the web center for the two webs immediately adjacent to the midchord (webs 3 and 4). The largest peak web stress (\approx 14,000 psi) was found to exist in web 3 and was a direct result of the low temperature measured at this point. This stress is 75 percent higher than the stress in web 4 and shows that for these test conditions the joint conductivity can have an important effect on the stresses. (See ref. 9.) Peak stresses for the other webs at the same spanwise station were between 8,000 and 10,000 psi with the 8,000-psi stress occurring in web 4. A somewhat above average value of joint conductivity is indicated in figure 10(b).

The skin stress histories at the bay centers were all similar, with peak stresses of about -3,000 psi. The maximum leading-edge stress, which occurred at 6 seconds test time, was calculated to be 740 psi; the maximum trailing-edge stress of 1,750 psi occurred at 9 seconds.

Comparison of calculated and experimental stresses.— Several significant facts are apparent from a comparison of the calculated stresses with the experimental-stress values obtained from the strain data for model MW-18. Both the experimental and calculated spanwise skin stresses have a magnitude of about -3,000 psi at the section 3 inches from the model tip. The strain gages also show that the chordwise stresses at this section were about 2,000 psi. This value of chordwise strain, considered with the low values of rib stress and small rib area (when compared with the skin area on a spanwise section), indicates that

some form of chordwise restraint, other than the ribs, was present. Such a restraint exists in a flat plate which is clamped at one edge and is subjected to a uniform temperature rise. (See ref. 10.) Calculations using the methods outlined in this reference indicate that the root restraint will induce chordwise stresses in the same range as those measured at a distance 3 inches from the tip of model MW-18.

The singularly high calculated peak stress in web 3 in model MW-18 is a direct consequence of the relatively low temperature measured at this location and probably results from a low, local joint conductivity which retarded the heat flow into the web. The joint conductivity may be expected to vary from one location to another, inasmuch as it is a function of such things as tightness of joint and contact-surface condition of materials (things which are difficult to evaluate on other than a statistical basis).

The low values of strain (when considered with the ratio of rib area to skin area) measured in the ribs show that the assumption that chordwise rib restraint could be neglected in the spanwise stress calculations was valid for these model tests. Inasmuch as the strain gages on the chordwise ribs in models MW-16, MW-17, and MW-18 indicated that these members contributed little thermal-stress restraint to the models, the stress calculations at the section 3 inches from the tip on model MW-18 should also apply to all the other models in this group provided the stresses are normalized with respect to the individual test conditions (with respect to the difference between the test stagnation temperature and the initial temperature of the model).

Discussion of Failure

The first test of model MW-4-(2), which occurred under conditions where aerodynamic heating was not present, showed that, although this design may be near-marginal, the model was strong enough to withstand the aerodynamic forces at a Mach number of 2 and sea-level static pressure and was stiff enough to resist flutter under these test conditions. The second test, made at a stagnation temperature of 5630 F, added thermal stresses due to aerodynamic heating to the stresses caused by aerodynamic loading and reduced the modulus of elasticity of the aluminum alloy. Both the thermal stress and the reduced modulus contributed to the decrease of the effective stiffness of the model; a chordwise flutter mode developed, and the model completely destroyed 0.36 second after the flutter mode began. The first model (model MW-4) of this design had been previously tested and had failed at 5.60 seconds after the start of the test (ref. 4): whereas model MW-4-(2) failed at 7.68 seconds after the start of the test. Other than the small difference in the time of failure, the two models failed in a very similar manner: both failed 0.36 second after the

beginning of the flutter mode; the flutter frequency of model MW-4 was 240 cps and that of model MW-4-(2) was 238 cps; and both models failed when the large distortions of the cross section crushed the tip rib.

A comparison of the test conditions of the two models shows that the thermal stresses in model MW-4 should be about 10 percent lower than those in model MW-4-(2) (see appendix of ref. 3); however, a comparison of the normalized temperature distributions between the two models leads to discrepancies which indicate that the methods used to determine aerodynamic test conditions did not give compatible values between the two sets of tests. In reference 4 two probes mounted on posts behind the model were used to measure the stagnation temperatures; whereas for the tests reported herein, probes mounted in the screen section just downstream from the jet settling chamber were used either exclusively or were averaged with the probes mounted behind the model. As a check, the experimental adiabatic-wall temperature was calculated for model MW-18 in run l by using the model temperature data (see ref. 4), and the stagnation temperature was then calculated by using a recovery factor of 0.88. The resulting stagnation temperature, as experienced by the model, was 480° F. which was considerably lower than the stagnation temperature of 523° F indicated by the tunnel data. The results, if the data agreement in figure 9 is used as justification, may be extrapolated to the elevatedtemperature test on MW-4-(2). The temperature comparison indicates that, if the stagnation temperature in the test on MW-4-(2) had been lower, better agreement would be found among the test data between the MW-4 design models: this would also have the effect of lowering the stress level in model MW-4-(2) to that in model MW-4. Thus, the small discrepancy in time of failure between the two models can be partly attributed to experimental error in determining the test conditions. A difference in joint conductivity between the two models also might have influenced the time of failure, but no reliable comparison between the models could be made since the only skin-and-web thermocouple combination available in model MW-4-(2) was near the root, a position where the parabolic-like stagnation-temperature profile across the jet stream would cause the temperature difference between these somewhat offset (spanwise) thermocouples to be questionable. (See fig. 3(a).)

Studies of a cross section of the MW-4 design show that the mode of cross-sectional distortion observed during the flutter of models MW-4 and MW-4-(2) may be induced by applying shearing loads to the skins in such a manner that the opposite skins tend to slide with respect to each other. (The same effect may be obtained by applying equal moments and equal and opposite forces at the leading and trailing edges, respectively.) If the riveted joints between the webs and the skins are replaced by pinned connections, the cross section in figure 1(a) becomes a series of four-bar linkages and will have no resistance to distortion; also, if the aforementioned loading is applied, the cross section will distort into a shape

approximating the distortion of the cross section during flutter. This shape is a direct result of the fact that the opposite skins are not parallel to each other (except at the center chord) but instead slope together. In the actual model, however, the skin is continuous and must bend when the cross section distorts; for ribless models, then, the skin bending stiffness is a criterion in determining the flutter resistance.

The major effect of the chordwise ribs in models MW-16, MW-17, and MW-18 was not to increase the skin bending stiffness but to restrain the chordwise distortion by preventing the skins from sliding past each other at points other than those at the leading and trailing edges. It may be possible to add sufficient restraint (for these test conditions) by using only a partial chordwise rib extending over one or two cells; if one or two cells are restrained, the effective stiffness of the entire cross section against this type of distortion is increased.

SUMMARY OF RESULTS

Four multiweb wing models of 20-inch chord and span with 0.064-inch-thick skin, 0.025-inch-thick ribs and webs, and zero, one, two, or three chordwise ribs were tested. The following results are given:

- 1. The model without chordwise ribs survived the first test where aerodynamic-heating effects were absent, but it failed during the second test when heating effects were included; thus, the present test confirmed the conclusions formed after an earlier test on another model of the same design (see NACA Research Memorandum L57HOl) that aerodynamic heating made the model susceptible to flutter.
- 2. The mode of flutter failure involved distortion of the entire cross section of the model, a condition which required that the individual cells of the model cross section distort and the opposite skins slide with respect to each other. Chordwise ribs helped to restrain this sliding tendency. One chordwise rib was sufficient to prevent flutter of this model design under these test conditions. The addition of one chordwise rib nearly doubled the lowest natural frequency at which chordwise deformation occurred.
- 3. The temperature data compared very well from model to model on a normalized basis.
- 4. The experimentally measured stresses were well below yield stresses for the aluminum alloy used in the model construction. The largest stresses were in the spanwise webs. Chordwise skin stresses near the model roots were larger than those elsewhere in the skin because of the

large restraint at this location. Direct rib stresses were small. The error in the measured strains is estimated to be about the same as the skin strains caused by thermal stresses.

5. The thermal stresses calculated for one model were in agreement with the measured stresses within the accuracy of the test data. The low strains measured in the chordwise ribs indicate that these calculations which neglect the restraint of ribs may be extrapolated to the other models with more or fewer ribs.

Langley Aeronautical Laboratory,
National Advisory Committee for Aeronautics,
Langley Field, Va., November 27, 1957.

3V

REFERENCES

- 1. Heldenfels, Richard R., Rosecrans, Richard, and Griffith, George E.:
 Test of an Aerodynamically Heated Multiweb Wing Structure (MW-1)
 in a Free Jet at Mach Number 2. NACA RM 153E27, 1953.
- 2. Griffith, George E., Miltonberger, Georgene H., and Rosecrans, Richard:
 Tests of Aerodynamically Heated Multiweb Wing Structures in a Free Jet
 at Mach Number 2 Two Aluminum-Alloy Models of 20-Inch Chord With
 0.064- and 0.081-Inch-Thick Skin. NACA RM L55F13, 1955.
- 3. Heldenfels Richard R., and Rosecrans, Richard: Preliminary Results of Supersonic-Jet Tests of Simplified Wing Structures. NACA RM L53E26a, 1953.
- 4. Rosecrans, Richard, Vosteen, Louis F., and Batdorf, William J., Jr.:
 Tests of Aerodynamically Heated Multiweb Wing Structures in a Free
 Jet at Mach Number 2 Three Aluminum-Alloy Models and One Steel
 Model of 20-Inch Chord and Span With Various Internal Structures
 and Skin Thicknesses. NACA RM L57HOl, 1957.
- 5. Miltonberger, Georgene H., Griffith, George E., and Davidson, John R.: Tests of Aerodynamically Heated Multiweb Wing Structures in a Free Jet at Mach Number 2 Two Aluminum-Alloy Models of 20-Inch Chord With 0.064-Inch-Thick Skin at Angles of Attack of 0° and ±2°. NACA RM L57H19, 1957.
- 6. Vosteen, Louis F., and Fuller, Kenneth E.: Behavior of a Cantilever Plate Under Rapid-Heating Conditions. NACA RM L55E2Oc, 1955.
- 7. Vosteen, Louis F., McWithey, Robert R., and Thompson, Robert G.:
 Effect of Transient Heating on Vibration Frequencies of Some Simple
 Wing Structures. NACA TN 4054, 1957.
- 8. Heldenfels, Richard R.: The Effect of Nonuniform Temperature Distributions on the Stresses and Distortions of Stiffened-Shell Structures.

 NACA TN 2240, 1950.
- 9. Griffith, George E., and Miltonberger, Georgene H.: Some Effects of Joint Conductivity on the Temperatures and Thermal Stresses in Aero-dynamically Heated Skin-Stiffener Combinations. NACA TN 3699, 1956.
- 10. Aleck, B. J.: Thermal Stresses in a Rectangular Plate Clamped Along an Edge. Jour. Appl. Mech., vol. 16, no. 2, June 1949, pp. 118-122.

NACA RM L57L13

TABLE I.- NATURAL VIBRATION MODES AND FREQUENCIES FOR MODELS

| | | | | F | requency, | cps, for n | ode line ^a | | | | |
|----------|------|-----|-----|-----|-----------|------------|-----------------------|-----|-----|-----|------|
| | А | В | С | D | E | F | G | Н | I | J | K |
| Model. | ,,,, | | | | | | | | | | 5.,, |
| MW-4-(2) | 72 | 144 | 268 | | 392 | | 427 | | 529 | | |
| MW-18 | 73 | 156 | | 326 | | 465 | | | | | 585 |
| MW-17 | 75 | 160 | | 335 | | 533 | | | | 746 | 661 |
| MW-16 | 70 | 147 | | 318 | | 554 | | 439 | | 747 | 677 |

Modes shown are composites from modes for all models. Individual modes varied slightly from those shown. Sketches show node lines obtained during room-temperature vibration tests.

TABLE II.- AERODYNAMIC-TEST-DATA SUMMARY GIVING AVERAGED TEST CONDITIONS

| Model | Test | Stagnation pressure, psia | Stagnation temperature, | Free-stream static pressure, psia | Free-stream dynamic pressure, psi | Free-stream temperature, o _F | Free-stream velocity, fps | Free-stream density, slugs/cu ft | Speed of sound, fps | Reynolds number per foot |
|----------|---------|---------------------------|--------------------------|--|--|---|----------------------------------|----------------------------------|--------------------------------|--------------------------------|
| MW-4-(2) | 1 2 | 110 | 93 563 | 14.3 15.1 | 39.8 41.7 | -152 111 | 1,713 2,330 | 3.90 × 10 ⁻³ | 861 | 27.7 × 10 ⁶ |
| MW-16 | 1 2 3 4 | 114 116 115 112 | 111 521 514 506 | 14.8 15.1 15.0 14.5 | 41.0 41.8 41.5 40.2 | -141 89 84 79 | 1,741 2,284 2,275 2,265 | 3.89 2.30 2.31 2.26 | 875 1,148 1,143 1,138 | 26.1 13.4 13.5 13.3 |
| MW-17 | 1 2 | 114 | 530 524 | 14.8 | 41.2 40.7 | 92 89 | 2,292 2,284 | 2.26 | 1,152 1,148 | 13.2 |
| MW-18 | 1 2 | 114 | 523 556 | 14.9 | 41.0 | 88 | 2,285 | 2.26 | 1,148 1,167 | 13.3 |

TABLE III.- MODEL TEMPERATURE HISTORIES

| | | t, | | | | | | | | | | | | Ter | nper | atur | e, º | F, at | t the | ermo | coup. | le ^a | | | | | | | | | | | |
|---------|------|---|--|--|--|--|--|---|--|--|--|--|---|---|--|---|--|--|--|---|--|--|---|--|--|--|---|--|---|---|--|--|--|
| Model | Test | sec | 1 | 2 | 1 | 3 | lı . | 5 | 6 | 7 | 8 | 9 | 10 | 11 | 12 | 13 | 14 | 15 | 16 | 17 | 18 | 19 | 20 | 21 | 22 | | | 25 | | | 28 | | 30 |
| W-4-(2) | 1 | 0 1 2 3 4 5 6 7 8 9 10 11 12 13 14 15 | | | 74 75 80 80 83 83 82 82 82 82 81 81 81 | | 80 81 83 81 80 79 79 77 76 77 75 | 79 83 88 84 84 84 82 81 82 81 80 80 80 | 80 83 86 87 83 84 83 83 83 82 82 80 80 79 | 78 79 82 85 83 83 82 83 81 81 81 79 79 | 77 78 82 82 83 84 82 80 80 81 79 80 81 | 81 84 83 81 82 83 82 81 81 81 81 81 | 81 86 88 81 86 85 81 82 81 82 80 80 79 81 | 79 83 85 85 81 82 82 82 81 80 79 78 79 78 | 79 82 82 85 84 83 82 80 81 79 79 79 78 79 | 78 81 82 83 83 82 81 80 80 79 80 79 | 78 81 80 83 83 84 82 82 81 80 81 81 81 | 79 78 79 81 80 81 82 81 82 82 80 81 80 81 | 79 78 80 81 81 81 79 78 78 77 76 75 73 74 72 | 83 84 88 87 86 86 84 83 83 83 83 81 81 82 | 84 86 90 86 85 83 81 81 79 80 79 78 77 78 77 | 82 81 88 87 81 83 82 80 81 79 79 78 78 77 | 83 85 87 87 86 85 82 82 80 81 80 81 | 81 81 82 79 77 76 71 71 73 72 71 71 69 68 70 | 82 82 81 79 78 77 75 75 70 70 69 71 | 77 78 79 80 83 81 82 81 81 79 80 79 79 79 | 82 79 79 79 78 78 78 80 81 81 80 81 81 85 83 | 81 86 85 86 85 83 83 83 83 87 79 83 79 | 82 85 88 87 84 83 83 81 80 78 78 78 78 78 | 88 91 93 91 88 88 87 81 82 82 83 82 82 82 | | 81 88 82 79 81 83 80 80 80 80 80 80 80 82 85 81 | |
| | 2 | 0 1 2 3 4 5 6 7 | 8 10 17 25 31 36 39 41 | 0 18 16 27 23 16 3 | 79 93 41 205 263 314 355 389 | | 86 122 188 249 293 327 351 371 | 83 | 82 129 193 254 300 337 366 390 | 80 95 135 190 239 282 320 351 | 78 82 98 133 180 226 271 308 | 81 127 191 250 293 331 361 385 | 82 126 193 254 301 336 366 389 | 83 118 174 230 271 307 336 362 | 79 95 134 181 231 268 301 331 | 80 97 135 182 226 265 299 328 | | 81 79 75 113 | 80 81 90 109 138 169 198 227 | 82 12h 182 237 282 316 345 369 | 86 123 193 250 294 329 358 381 | 79 118 187 244 287 322 350 374 | | 80 112 165 211 245 271 292 308 | 75 108 156 200 235 260 283 300 | | | | 8l ₄ 116 183 226 261 289 313 335 | 85 118 191 240 280 311 338 362 | | | 79 91 141 178 210 239 269 28 |
| | 1 | 0 1 2 3 4 5 6 7 8 9 10 11 12 13 14 15 | 8 9 9 9 9 9 9 9 9 9 9 9 9 9 9 9 9 9 9 9 | 33 35 35 32 32 32 32 32 32 32 32 33 39 39 39 39 39 39 39 39 39 39 39 39 | 82 84 87 89 90 91 90 90 90 89 90 89 88 88 88 | 88 93 95 96 94 93 93 93 93 91 91 91 90 89 | 88 87 88 | 814 83 83 82 82 82 81 81 80 80 | | 90 95 97 97 95 94 94 93 92 91 90 90 90 | | | | 82 83 84 86 87 87 88 87 88 87 86 86 86 86 | 82 81 83 85 85 85 81 81 81 81 81 | 94 92 91 90 89 88 88 87 86 86 | 86 90 90 89 88 87 86 86 85 84 84 84 | 87 89 91 88 86 85 83 82 82 80 80 79 78 78 | 84 87 87 86 84 83 82 81 80 79 78 75 75 | 87 86 84 84 83 82 81 81 | 92 91 91 90 89 88 88 88 88 | 85 84 83 83 83 82 | 86 87 89 90 91 91 91 90 89 88 88 90 88 | 87 86 86 85 85 86 85 | 78 79 79 79 87 | 88 88 87 87 87 87 87 | 87 85 86 86 86 86 86 86 86 | | 87 90 94 93 91 91 89 90 89 89 89 88 88 88 | 88 89 89 88 87 86 86 86 86 86 | 85 86 89 90 89 89 88 88 87 87 87 87 | 85 86 90 90 89 88 88 88 87 86 88 88 87 86 | 8 8 9 9 8 8 8 8 8 8 8 8 8 8 8 8 8 8 8 8 |
| | 2 | 0 1 2 3 1 4 5 6 7 8 9 10 11 12 13 14 15 16 | 10 12 22 33 33 44 44 44 44 44 44 44 44 44 44 44 | 39 93 34 87 05 17 27 35 40 47 | 81 91 128 180 229 273 309 338 363 382 397 410 419 426 431 431 434 435 | 85 126 183 245 293 331 357 380 396 409 419 433 435 435 435 | 371 388 402 412 413 428 428 430 431 | 101 139 185 185 2 220 6 248 8 284 2 297 2 307 3 315 3 321 3 321 3 321 3 321 3 321 3 321 3 321 | 85 108 153 202 248 280 317 343 363 379 409 4109 4117 421 | 127 192 253 298 333 360 380 396 408 418 424 430 434 427 | | 78 82 93 117 150 18h 219 276 300 321 339 350 36h 375 376 | 79 145 191 232 264 290 316 336 352 364 376 387 394 406 | | 777 822 85 102 125 151 177 200 222 214 255 271 281 299 303 | 121 185 238 279 311 337 358 2387 387 398 441 413 417 410 | 116 180 233 307 333 354 371 385 391 406 413 419 | 183 211 237 256 271 283 298 300 307 311 311 311 308 | 218 241 263 278 292 301 309 319 320 309 309 309 309 | 82 89 107 129 15L 178 201 2222 | 115 171 219 256 287 311 331 | 238 289 324 349 369 384 396 405 411 425 432 432 432 432 432 432 432 432 432 432 | 148 178 202 229 252 273 291 308 321 337 352 361 | 81 93 115 143 173 202 228 252 275 293 311 325 340 2353 4362 | | | 84 114 171 210 214 272 292 316 334 350 363 373 382 396 389 386 | | 83 109 160 191 226 267 286 307 321 337 351 363 383 383 | 88 113 1143 170 170 8 196 8 240 7 259 1 277 7 293 1 308 3 323 3 341 3 351 1 360 | 227 250 269 287 305 319 334 352 364 368 | 22L 24L 267 287 305 321 335 350 367 375 377 | 166 159 222 259 271 259 311 323 313 313 313 313 313 313 313 313 |
| MW-16 | 3 | | 2 1 2 2 3 3 3 3 3 3 3 3 3 3 3 3 3 3 3 3 | 74, 95, 51, 15, 65, 101, 134, 158, 177, 192, 103, 112, 125, 125, 125, | | 259 321 34 366 380 390 400 41 | 126 186 246 286 316 366 37 366 37 366 37 38 39 40 41 41 | 0 90 6 1hi 18i 7 21 9 23i 3 25i 3 27i 7 28i 9 29i 8 29i 6 30i 6 30i 6 30i 7 30i | 6 76 96 139 181 220 5 261 1 291 2 32 3 34 9 361 4 37 9 38 2 39 8 39 | 5 111 5 167 220 263 299 327 386 397 409 411 600 600 600 600 600 600 600 6 | 77 22 1 57 7 7 7 7 7 7 7 7 7 7 7 7 7 7 7 7 7 | | 76 75 138 181 215 241 273 296 316 357 365 376 | 7 17: 3 20: 3 28: 3 28: 3 28: 3 28: 3 28: 3 31: 3 35: 3 36: 3 | 8 7 8 8 9 9 1 12 3 1 1 1 7 1 7 1 9 1 9 2 1 2 3 2 5 7 2 7 3 2 8 2 9 2 9 1 2 9 1 2 9 | 10 10 10 180 180 180 180 180 180 180 180 | 7 101 0 171 1 220 0 260 1 281 7 315 8 336 8 360 380 390 100 5 110 | 3 103 3 143 178 2 209 7 226 5 246 5 265 2 26 2 29 0 29 8 30 3 30 1 30 | 1 101 138 177 2 206 2 26 2 26 2 26 2 26 2 26 2 29 3 29 3 29 1 29 1 29 | 1 79 88 82 7 100 6 122 88 116 9 169 169 169 169 255 225 225 227 23 24 25 25 27 28 28 28 28 | 5 107 168 211 2 250 6 27 9 30 9 32 9 32 10 34 13 36 8 37 2 38 2 38 9 40 | 7 131 220 1 266 297 8 318 3 338 1 357 1 365 1 37 1 38 1 38 2 39 9 39 | 85 100 7 135 8 166 8 19 8 21 2 23 2 27 8 29 8 29 31 7 32 0 33 | 71 86 81 101 131 131 14 155 11 18 21 23 25 26 29 29 31 32 31 32 33 32 33 34 34 35 36 36 36 36 36 36 36 36 36 36 36 36 36 | 77 73 77 99 83 33 33 33 34 11 | | 71 103 165 201 238 266 289 309 321 311 359 361 378 390 391 381 | 77 | 70 1hl 17! 200 22: 2h 26: 29: 31 32: 33: 35: 36: 35: | 0 4 5 4 7 7 2 4 6 1 | 73 78 107 138 166 193 217 238 250 277 293 308 336 356 | 85 121 156 18 20 23 25 27 28 30 31 33 31 36 36 | 111222223333333333333333333333333333333 |
| | 1 | + | 1 2 3 4 5 6 7 8 9 9 0 1 1 2 3 4 4 5 6 | 277 314 342 365 382 396 407 415 426 425 | 130 177 22h 263 296 32h 346 369 380 392 401 409 413 | 121 25 28 31 35 37 38 39 40 41 41 | 137 70 25 3 29 9 32 7 35 7 38 3 39 10 14 14 14 14 14 18 | 15 10 17 11 15 19 18 22 18 24 13 26 11 27 15 28 16 29 15 30 11 30 17 31 17 31 | 682264876493266 | 89 121 17 22 27 30 33 35 37 39 h0 h1 h1 h2 | 4573857733285 | | 38 38 38 | 5 8 8 9 2 11 0 13 1 17 9 20 8 23 7 25 4 30 0 32 6 33 0 34 7 35 8 35 | 6 8 3 8 2 10 8 12 0 14 2 17 1 19 8 21 2 23 3 24 0 26 3 26 | 2 12 7 18 4 23 2 27 5 30 3 34 3 36 3 37 3 38 6 39 7 40 8 41 | 3 11 3 17 2 26 3 29 7 31 6 34 2 35 7 38 6 39 1 39 0 40 | 6 10 8 14 17 20 1 22 9 24 9 25 7 26 1 28 1 28 1 28 1 28 1 28 1 28 1 28 1 28 | 6 10 4 14 9 18 6 21 7 23 3 25 7 26 8 27 7 28 29 29 29 29 29 28 8 28 6 28 | 7 8 9 1 10 0 12 2 14 0 16 5 18 5 20 1 23 7 25 6 7 27 8 27 | 3 11 0 17 7 21 7 25 8 27 8 30 8 32 6 33 1 35 6 36 30 30 36 30 36 30 30 36 30 3 | 0 22 4 27 1 30 9 32 3 34 2 36 7 37 1 38 8 39 7 40 3 40 4 38 | 6 8 3 10 2 11 4 14 7 17 6 19 0 21 1 24 1 26 9 28 6 29 2 30 6 32 0 33 | 8 8 9 9 9 8 11 16 19 9 21 23 3 25 0 27 6 29 | 7661850578 5 1591 | | 86 11 166 20 24 26 29 31 32 34 35 36 37 38 37 | 3991 771 1061 1346 77 | 29 30 31 33 34 36 36 | 2 9 7 11 6 14 2 16 4 19 5 21 4 25 7 26 9 28 1 29 6 31 1 32 | 90 11 14 8 17 2 20 2 22 3 24 1 26 8 27 7 30 1 32 8 33 6 34 | 7 13 3 16 4 19 2 21 3 23 4 25 1 27 7 28 3 30 7 31 8 34 8 34 | 1 1 1 1 1 1 1 1 1 1 1 1 1 1 1 1 1 1 1 |

^aBlanks in data denote that the instrument was not used.

TABLE III .- MODEL TEMPERATURE HISTORIES - Concluded

| | | t t | I | | | | | | | | | | | | | Te | mper | atur | e, o | F, a | t th | ermo | coup | lea | - | | | | | | | | | | | | |
|-------|-----|---|------|---|---|---|---|---|---|--|--|---|--|---|---|---|---|---|--|---|--|--|---|--|---|--|---|---|--|--|---|--|--|--|---|---|---|
| Model | Tes | se | | . 2 | | 3 | 4 | 5 | 6 | 7 | 8 | 9 | 10 | 11 | 12 | 13 | 14 | 15 | 16 | 17 | 18 | 19 | 20 | 21 | 22 | 23 | 24 | 25 | 26 | 27 | 28 | 29 | 30 | 32 | 33 | 34 | 35 |
| | 1 | 0 1 2 3 4 5 6 7 8 9 10 11 12 13 14 15 | | 16 1 195 1 263 2 309 2 314 2 371 2 390 2 104 3 117 3 117 3 1137 3 1139 3 1139 3 | 66 84 98 10 119 124 128 | 156 190 219 245 261 281 294 304 311 318 321 | | 317 320 321 315 | 124 156 185 210 231 247 260 271 281 289 295 | 290 298 306 311 314 | 68 92 130 168 197 222 243 257 270 280 291 296 301 301 299 299 | 279 290 298 305 310 | 139 172 203 232 259 281 300 316 330 342 352 | 60 67 78 103 134 167 200 231 257 283 305 324 335 | 69 70 78 93 116 139 162 184 203 220 235 248 257 267 274 277 | 228 269 302 329 352 370 384 395 406 412 | 171 224 265 297 324 348 365 380 391 402 409 | 379 389 397 1,02 | 69 101 170 217 254 284 309 331 346 361 375 386 392 405 403 | 72 106 167 211 248 276 301 323 341 358 369 380 388 393 400 399 | 383 389 395 | 71 105 166 218 259 291 318 339 356 371 384 393 400 409 408 | 208 246 277 302 323 340 356 367 377 385 390 | 214 252 283 309 329 345 360 369 377 387 386 | 171 198 222 240 255 267 | 300 | 123 150 177 203 227 248 269 285 304 320 333 | 162 193 222 248 270 292 310 327 338 355 | 89 112 136 159 182 200 220 235 248 260 268 274 | 168 196 220 238 252 265 276 283 290 295 288 286 | 90 113 145 181 214 242 281 293 313 329 344 355 | | 205 230 254 274 291 308 324 360 | 133 167 194 217 236 251 263 274 281 289 281 284 | 294 315 333 350 362 374 385 398 397 | 206 239 265 288 | 201 221 231 245 262 267 267 267 263 |
| MW-17 | 2 | 23 33 44 56 77 88 99 10 11 12 13 14 15 | | 87 136 1209 1272 315 3148 374 393 407 419 429 4435 440 440 441 | 87 118 169 212 245 267 284 296 307 331 3327 3331 3325 | 83 87 102 131 163 193 220 212 260 | | 296 304 311 316 319 319 316 | 231 248 261 | 113 156 195 224 246 265 280 291 300 307 312 316 314 312 | 273 284 291 297 302 302 | 135 165 192 217 256 271 284 295 303 309 314 317 | 150 182 211 239 264 286 304 321 334 346 | | 85 86 93 109 130 150 171 191 208 224 237 248 259 268 271 277 | 181 232 272 305 331 352 369 384 405 411 422 | 178 229 268 300 326 347 365 379 391 402 408 418 | 226 262 291 | 179 224 258 287 311 331 349 364 374 385 392 401 402 | 1372 | 123 183 227 261 290 314 334 363 374 382 390 398 | 179 226 263 294 319 356 371 382 391 398 403 407 | 122 171 215 251 280 304 323 342 355 368 377 38h | 120 | 86 109 114 178 205 227 244 259 272 281 290 295 300 295 294 293 | 212 | 80 85 92 106 122 142 164 189 211 232 252 271 289 307 327 322 | 1144 174 202 230 2514 277 296 3114 330 3141 | 84 89 104 123 145 166 187 208 224 241 253 265 273 276 | 145 179 205 227 243 257 270 278 286 292 295 | 100 118 141 164 189 216 255 285 305 323 336 353 365 383 | 108 148 185 218 218 274 297 317 334 349 362 376 384 391 | | 222 239 253 266 275 284 289 285 285 286 | 180 217 249 276 298 317 334 350 363 373 387 399 393 | | 139 168 190 208 223 234 246 255 262 265 257 263 266 |
| | 1 | 2 3 3 1 5 6 7 8 9 10 11 12 13 11 15 15 15 15 15 15 15 15 15 15 15 15 | | 201 266 313 348 376 376 412 425 436 4449 | 77 111 164 210 243 268 300 310 3319 3325 3335 3335 3335 3335 | | 78 81 95 125 163 202 239 272 303 328 350 368 384 397 405 401 | | | 248 290 326 352 373 391 405 416 426 431 | 122 186 243 282 316 342 362 380 394 405 413 418 422 420 | 121 183 238 281 314 340 363 382 395 406 415 421 | | 157 201 234 261 281 297 311 329 336 339 | 105 159 205 244 278 308 334 357 376 390 403 412 | 88 98 118 142 170 198 224 249 273 297 312 | 119 153 187 219 251 278 304 324 342 356 370 | 91 120 155 194 230 262 291 318 339 357 371 383 | 78 87 103 128 153 179 202 224 242 257 271 282 | 80 11h 182 23h 275 30h 329 350 367 383 395 hoh h12 h22 h17 | | | 84 120 180 230 269 300 326 347 363 377 388 398 402 407 | 118 180 231 270 302 328 348 364 377 390 398 404 | 90 103 122 143 167 192 217 240 260 281 299 | 226 264 293 317 336 355 370 382 391 398 | 260 292 317 338 355 368 379 387 392 | 184 213 238 257 271 285 294 302 308 312 308 | 103 142 181 211 237 256 273 285 297 305 315 316 | 139 173 212 250 284 293 319 344 368 375 381 | 81 89 104 125 150 173 196 216 235 252 | 176 228 266 300 326 348 367 382 395 406 415 | 83 102 137 184 224 256 284 310 329 345 357 368 389 396 398 | 103 129 160 191 220 247 270 290 310 328 342 354 | 113 175 212 245 272 297 317 335 351 364 375 387 400 | 116 182 222 255 282 305 326 345 360 372 384 396 409 | 146 176 199 219 236 256 26 27 286 289 299 299 |
| MW-18 | 2 | 100 | 2233 | | 78 113 174 226 261 286 307 324 3345 3352 357 361 361 3358 | | 128 161 195 228 258 284 307 329 352 389 410 | 77 92 126 168 210 250 | | | 246 291 328 357 378 397 412 425 436 | 118 186 248 294 331 361 385 405 419 431 441 449 453 | 119 182 241 285 321 349 371 389 401 413 422 427 | 164 213 251 279 302 321 334 347 356 362 368 370 363 | 98 155 204 248 285 318 346 371 390 406 420 441 441 | | 74 77 92 118 154 192 229 262 291 320 341 361 377 392 405 410 | | | 112 188 245 288 320 347 367 367 405 415 424 | | | | 76 116 185 243 286 320 347 369 386 402 413 421 421 432 436 | | 393 406 418 428 434 437 441 | 229 270 305 333 356 375 389 403 411 419 425 | 307 319 327 334 338 336 334 | 103 | | 77 79 86 98 117 141 165 190 214 253 271 285 300 309 314 | | 275 302 326 348 365 382 | 78 96 124 158 190 250 275 298 319 337 354 370 | 168 210 247 279 304 327 345 366 378 390 402 417 420 | 108 182 226 262 293 318 341 359 375 390 401 | 107 151 185 212 231 251 266 280 291 307 311 312 315 |

^aBlanks in data denote that the instrument was not used.

| | | | | | | | | | | | | | ch. at | strain | 28.20 | locati | ona | | 1000 | | |
|----------|------|--|--|---|---|--|---|--|--|--|--|--|--|---|--|--|---|--|--|---|---|
| Model | Test | t, sec | 1 | 2 | 3 | 4 | 5 | 6 | 7 | 8 | 9 | 10 | 11 | 12 | 13 | 14 | 15 | 16 | 17 | 18 | 19 |
| MW-4-(2) | 1 | 0 1 2 3 4 5 6 7 8 9 10 11 12 13 14 15 | | 14 -91 -95 - 8 14 65 14 65 16 17 -21 -110 -237 - 17 12 | | | | -7 -32 -10 -7 0 5 2 0 0 7 17 2 8 27 | 2 62 -99 -45 -54 -73 -77 -86 -101 -170 -198 144 -54 -172 -21 | -8 -57 63 49 61 73 61 71 71 71 113 26 105 | -36 36 -100 -34 -24 0 2 17 19 15 -32 -24 86 73 19 | 2 - 255 - 255 - 255 - 350 - 35 | 8 149 -259 -206 -213 -212 -219 -223 -2114 -336 -261 -36 -166 -623 -162 | 15 -36 314 -23 -61 -63 -80 -79 -77 -73 -63 -138 -71 -33 -65 | -l ₄ -58 -93 -25 -2l ₄ -18 -29 -36 -31 -l ₁ 9 -8l ₄ -73 -l ₄ l ₄ -73 | 2 -51 -103 -125 -133 | | | -4 13 -57 -2 0 13 -2 -2 4 8 8 -h2 -46 -46 | | |
| | 2 | 0 1 2 3 4 5 6 7 | | 388 297 212 115 87 84 72 | 17 360 930 1285 1393 1374 1283 1140 | | 17 103 238 215 145 131 131 189 | | | | -22 -160 -462 -701 -908 -1058 -1069 -994 | 12 222 330 290 199 143 75 14 | 8 -55 -6 -29 -129 -230 -273 -298 | | | | | | | | |
| | 1 | 0 1 2 3 4 5 6 7 8 9 10 11 12 13 14 15 | 13 73 105 202 192 170 164 143 119 96 55 52 -66 23 40 | 0 -40 -96 -42 -42 -4 23 2 19 12 23 -19 -35 -29 27 36 | -17 75 93 155 159 168 170 155 151 122 52 -14 56 97 83 | 4 35 6 57 64 62 66 39 31 37 21 -90 27 -92 -21 | | 23 90 75 81 49 36 32 21 19 6 -15 -34 45 9 58 | | -44 00 40 -199 -155 11 34 61 91 67 36 17 0 | 77 12h 122 112 11h 105 99 110 170 143 -46 149 165 | | | -6 0 -8 27 -8 11 27 33 23 33 263 121 270 -2 | 4 24 -49 -77 -88 -82 -97 -84 -80 -101 -110 339 15 5 | 8 17 -9 -11 -19 -24 -32 -26 -23 -24 -43 23 86 -11 | 2 -64 -185 -123 -167 -229 -209 -253 -161 -159 -169 -112 -237 -127 -127 | 40 -125 -63 -87 -79 -161 -146 -179 -88 -102 -56 15 -92 10 2 | 0 7 -15h -145 -139 -177 -225 -226 -237 -139 -170 -188 -132 -91 -4 5 | | |
| ₩-16 | 2 | 0 1 2 3 4 5 6 7 8 9 10 11 12 13 14 15 16 | | | | 2 13 130 70 50 57 48 29 32 48 57 95 78 63 -30 99 107 | | 22 327 760 1026 1085 1039 9hh 805 651 h87 320 1h7 -15 -91 -121 -217 | | 19 68 236 243 239 192 177 287 363 365 298 239 226 625 | 137 33 -90 -153 -185 -161 -133 -9h -46 | | 1 | | | | 2 32 107 151 155 135 111 62 24 -66 -177 -232 -228 -161 -139 -226 -254 | | 0 122 -7 -46 -122 -161 -135 -89 -68 -11 -51 -35 307 96 | 210 hh -2 -12 -6 -13 0 2 5h 110 158 h16 325 | |
| | 3 | 0 1 2 3 4 5 6 7 8 9 10 11 12 13 14 15 | | | | -9 44 87 47 59 87 118 117 120 130 134 125 122 70 132 104 | | 21 300 709 914 968 932 845 727 614 477 348 216 102 -18 -43 | | | -4 96 101 62 42 5 -16 -52 -56 -47 -40 -514 -63 -83 | | | | | | 2 314 153 194 195 189 168 140 116 94 80 76 83 172 236 166 | 5 2h 102 138 145 133 112 73 22 -10 -37 -66 -87 43 -31 -61 | | | 62 83 61 26 -10 -26 -23 -36 11 11 16; |
| | 14 | 0 1 2 3 4 5 6 7 8 9 10 11 12 13 14 | | | | -14 83 31 17 36 61 90 83 90 92 85 80 58 -134 63 | Y | 9 261 683 895 948 902 822 704 591 477 371 259 161 -159 70 | | | -5 113 57 19 -14 -26 -17 -10 17 36 15 38 8h -278 -46 | | | | | | 146 141 188 207 188 172 161 154 163 176 196 337 62 289 | 72 116 125 114 93 58 28 4 -7 -9 132 | | | |

^aDashes in data denote that the instrument failed or was deemed unreliable; blanks denote that the instrument was not used; and negative signs indicate compression.

TABLE IV. - MODEL STRAIN HISTORIES - Concluded

| | | 1 | t, | | | | 1 | | | Strai | | croin | ches p | er inc | | | - | - | - | | -0 1 | 70 1 | 001 | 07 |
|-------|------|----|--|---|--|--|---|--|--|---|--|--|---|--|---|---|---|----|---|---|---|---|---|---|
| Model | Test | se | ec | 1 | 22 | 3 | 4 | 5 | 6 | 7. | 8 | 9 | 10 | 11 | 12 | 13 | 14 | 15 | 16 | 17 | 18 | 19 | 20 | 21 |
| | 1 | | 0 1 2 3 4 5 6 7 8 9 10 11 12 13 14 15 | 312 186 111 254 239 162 | -13 -228 -287 -462 -143 -129 -529 -291 -150 -86 -361 -162 -106 8 | 0 165 251 233 196 131 151 645 | 543 805 897 | 22 -155 225 208 185 159 138 112 123 152 161 238 | -23 - -14 - -108 - -171 - -198 - -181 - -108 - | -306 -260 -304 -314 -273 -246 -154 -231 | -643 | -6 -52 -119 -208 -233 -260 -245 -237 -165 -10 31 148 66 231 299 389 | -18 -47 -251 -402 -493 -552 -561 -566 -533 -524 -488 -481 -373 -282 -260 | 4 -156 -141 -170 -168 -202 -226 -252 -274 -278 -285 -280 -313 -300 -256 -263 | 17 1144 267 275 264 239 243 211 213 206 174 116 80 39 -19 -146 | | | | | | 125 91 77 62 36 45 11h -12 0 18 161 16h 351 378 423 | -120 210 220 212 170 168 152 162 224 228 266 264 741 322 | | -11 -78 -85 -91 -33 6 26 46 126 150 179 205 277 214 |
| MW-17 | . 2 | | 0 1 2 3 4 5 6 7 8 9 10 11 12 13 14 15 | 2 385 331 303 281 | -15 -240 -209 -249 -211 -200 -238 -198 -225 -267 -273 -253 -320 -262 185 | -1440 | 910 887 833 772 709 653 588 487 388 337 | | 2) 129 55 26 -4 -38 -56 -89 -144 -186 -133 -122 75 -15 -14 71 | | -16 80 94 68 16 -17 -14 -30 -31 35 26 30 10 278 71 | -115 -59 -78 -30 24 95 | -34 -153 -333 -1548 -518 -6142 -705 -748 -790 -817 -851 -893 -982 -881 -787 | 512 | -12 252 323 305 305 293 286 277 235 236 222 201 219 319 -362 139 | 5 209 475 666 731 738 677 615 559 495 439 385 316 236 205 | | | | -4 22 93 122 135 139 117 104 75 40 9 4 20 36 57 22 | -7 74 55 44 52 23 30 22 -8 -28 -20 49 166 75 | | | -23 -110 -166 -110 -9h -135 -107 -86 -2h -28 -24 21 58 12 383 77 |
| | | 1 | 0 1 2 3 4 5 6 7 8 9 10 11 12 13 14 15 | 18 375 256 279 39 -107 -122 -172 -296 -213 -286 -345 -161 -271 | -93 -312 -276 -316 -145 -171 -52 -47 44 33 109 171 91 | | -21 26 -122 -166 -155 -122 -103 -96 -78 -66 -51 -55 -80 | 30000 | 20 285 616 861 909 892 834 758 672 578 502 416 329 127 -180 | -86 318 350 343 306 197 238 265 238 227 350 64 | 7 | -7 -40 -99 -203 -238 -261 -186 -144 -66 -72 -20 -71 18 59 -88 | -264 -411 -458 -519 -556 -590 -611 -612 -561 -561 -563 -780 -780 -399 | 56 12 -21 -39 5-55 -62 -60 -76 -76 -76 -76 -76 -76 -76 -76 -76 -76 | 59 -16 -122 62 | | -13 -225 -497 -524 -381 -265 -123 -30 188 55 120 161 195 225 | | 8 5 83 140 171 193 208 211 217 222 201 193 189 239 254 506 | -14 69 20 18 28 26 -12 -46 -57 -75 18 24 218 1445 | 248 363 | -25 84 125 | | -7 101 -61 -40 37 7 9 9 10 11 120 146 167 17 199 180 |
| MW-18 | | 2 | 0 1 2 3 4 5 6 7 8 9 10 11 12 13 14 15 | | -21 -335 -291 -215 -100 75 265 316 255 29 49 51 47 | 71.22.1.61.33.44.22.33 | 13 | 9041398918365 | 18 314 711 965 104 102 95: 83: 73: 633 55: 166 25 16 | 773332241111333 | | | -5. -200 -lul -55. -65 -70 -73 -75 -76 -77 -78 -67 -89 -86 -72 -82 | 175 88 90 21 33 -28 33 -28 -36 -14 -14 -14 -14 -2 -3 -3 -3 -3 -3 -3 -3 -3 -3 -3 | 32h 32h 32h 32h 32h 32h 32h 32h | 373 737 858 2 1089 2 1089 2 1089 3 900 789 6 682 5 77 46. | | | 3 2 63 114 147 177 199 2255 285 309 321 348 609 669 | | | | -21 -70 -100 -18: -25: -32: -37: -42 -43 -46 -47 -49 -49 -40 | 2 |

BDashes in data denote that the instrument failed or was deemed unreliable; blanks denote that the instrument was not used:, and negative signs indicate compression.

TABLE V.- SUMMARY OF MODEL BEHAVIOR

(a) Description of model-vibration tests

| Model | Test | Model vibration |
|-----------|------|---|
| 151 h (0) | 1 | 65-cps bending and torsion after starting disturbances; 130-cps random vibration at 8.7 seconds; 80-cps torsion at 10.7 seconds; 173-cps torsion after tip-stabilizer reentry |
| MW-4-(2) | 2 | 72-cps vibration after starting disturbances; 238-cps flutter until destruction between 7.32 seconds and 7.68 seconds |
| | 1 | 60- to 78-cps random vibrations throughout test |
| MW-16 | 2 | 275- to 286-cps random vibrations throughout test; 60-cps vibration before shutdown disturbances |
| | 3 | 258- to 266-cps random vibrations throughout test |
| | 14 | 60-cps vibration at 9 seconds |
| MW-17 | 1 | 130- to 140-cps vibrations throughout test; 140-cps torsion after tip-stabilizer reentry |
| | 2 | 140-cps torsion after tip-stabilizer reentry |
| | 1 | 145-cps bending and torsion after tip-stabilizer reentry |
| MW-18 | 2 | 70-cps vibration from 5 seconds until shutdown; 124- and 70-cps torsion after tip-stabilizer reentry |

(b) Approximate times for particular events

| Approximate time, sec | Stagnation pressure, psia | Model condition |
|-----------------------|---------------------------|---------------------------------|
| 0 to 1.2 | <50 | Violent model buffeting |
| 1.7 to 11.5 | >100 | Test conditions exist |
| 1.7 to 11.0 | | Tip stabilizer out of airstream |
| 13.4 to end | <50 | Violent model buffeting |

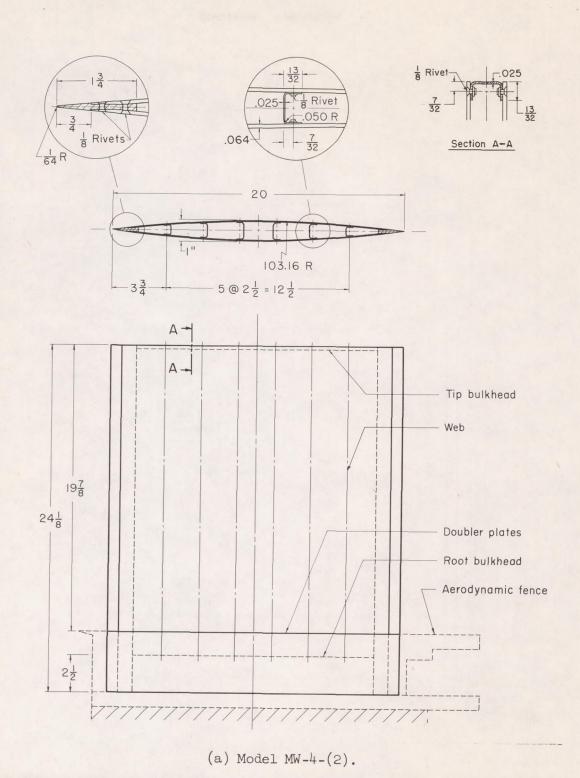
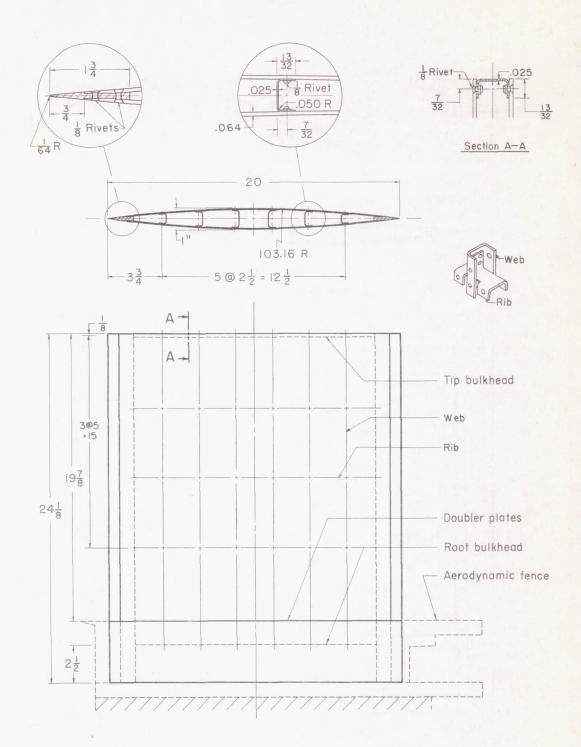
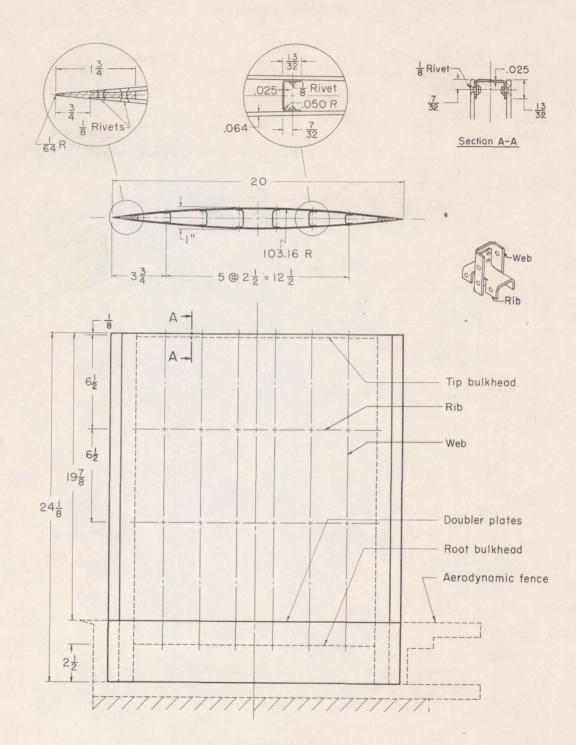


Figure 1.- Construction of multiweb wing models. All dimensions are in inches.



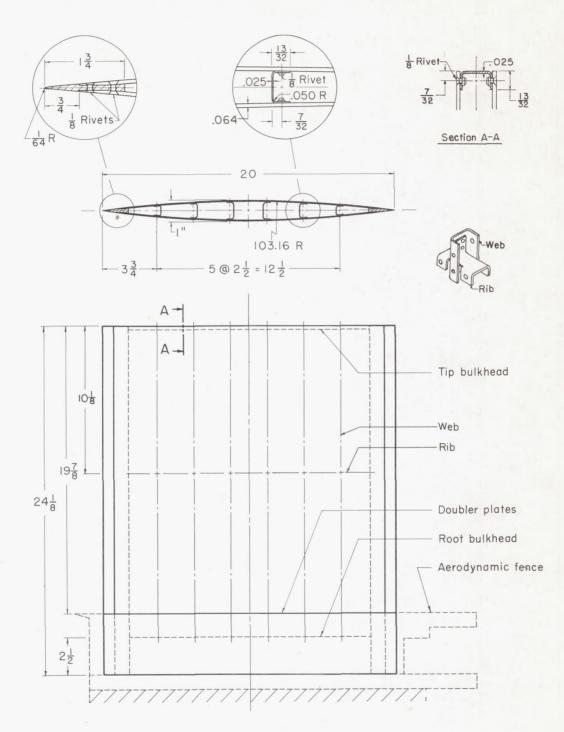
(b) Model MW-16.

Figure 1. - Continued.



(c) Model MW-17.

Figure 1. - Continued.



(d) Model MW-18.

Figure 1.- Concluded.

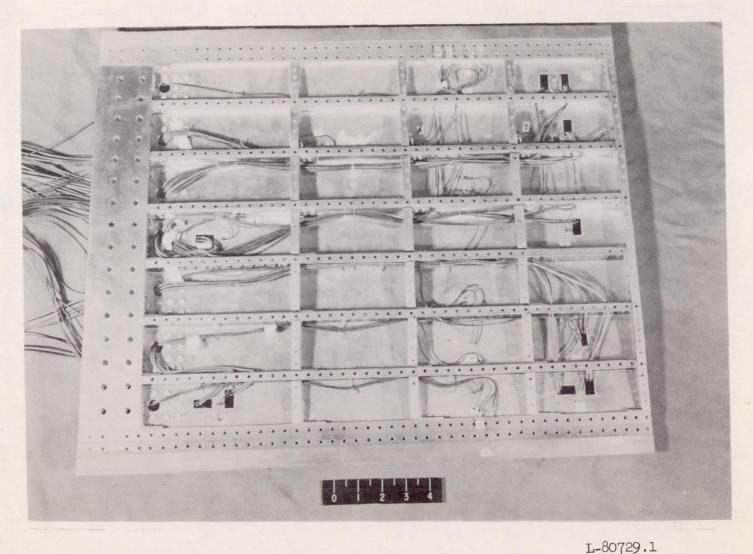
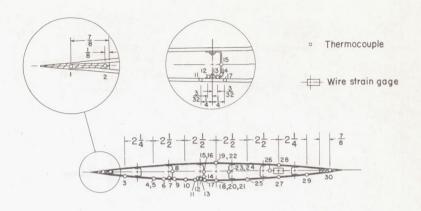
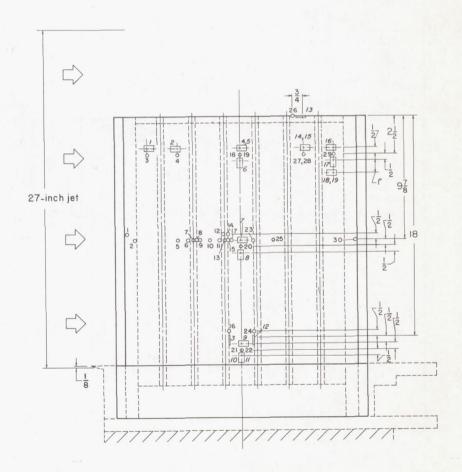


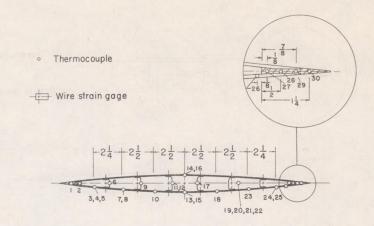
Figure 2.- Photograph showing installed instrumentation in interior of model MW-16 prior to final assembly.

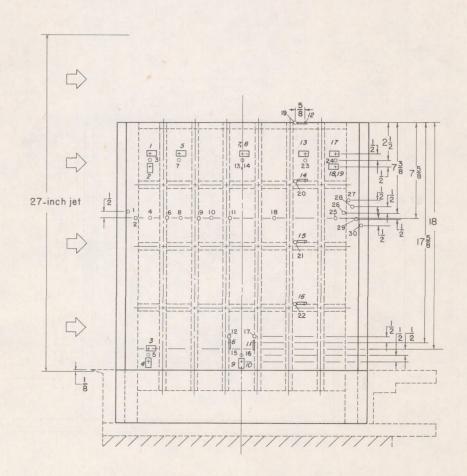




(a) Model MW-4-(2).

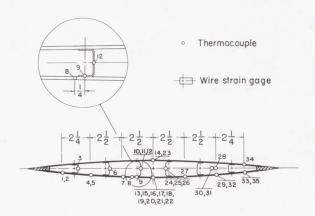
Figure 3.- Location of instrumentation of multiweb wing models. Where two wire strain gages are listed, the second is on the far skin.

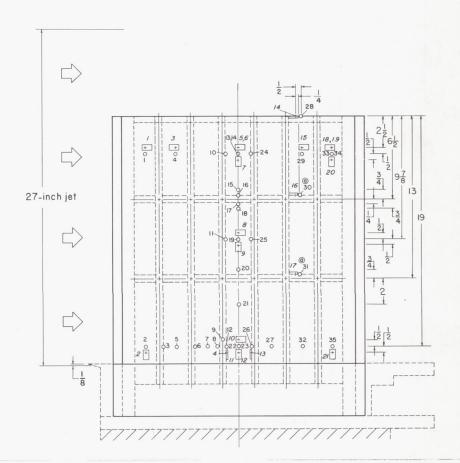




(b) Model MW-16.

Figure 3. - Continued.



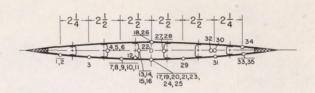


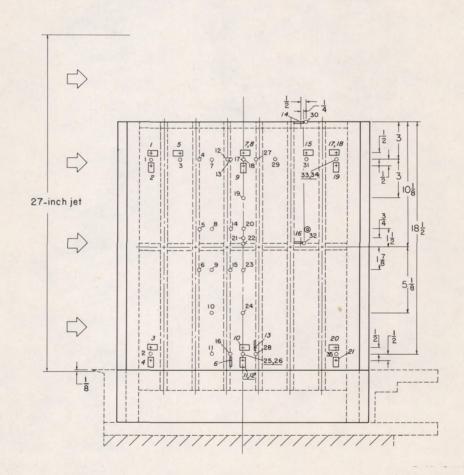
(c) Model MW-17. The symbol (a) denotes a dimension of 3/8 inch between thermocouple and wire-strain-gage center line.

Figure 3.- Continued.

Thermocouple

Wire strain gage





(d) Model MW-18. The symbol (a) denotes a dimension of 3/8 inch between thermocouple and wire-strain-gage center line.

Figure 3. - Concluded.

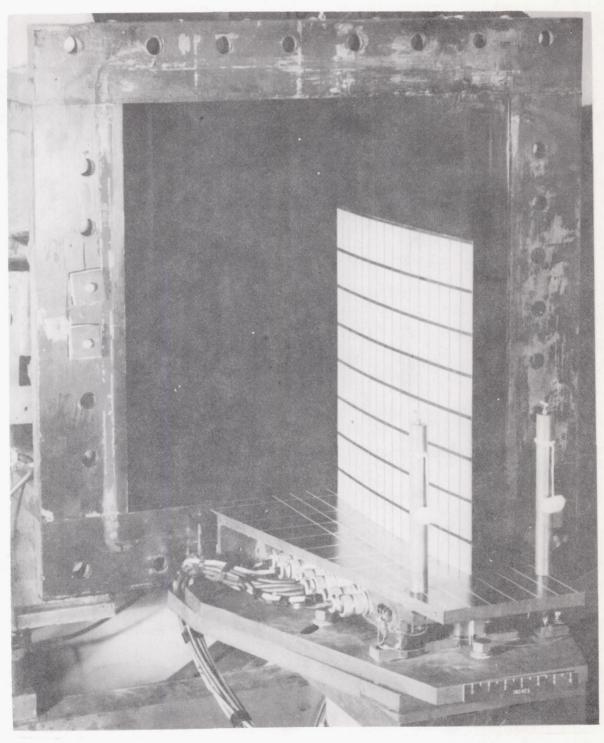


Figure 4.- Model in place at nozzle exit prior to test. L-81922

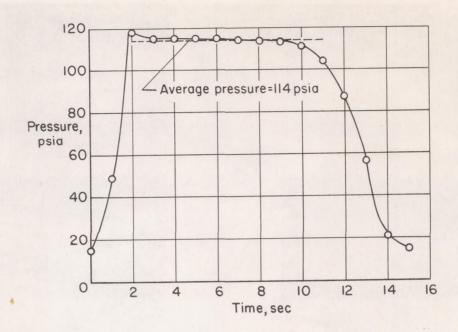


Figure 5.- Typical variation of stagnation pressure with time.

Model MW-18; test 1.

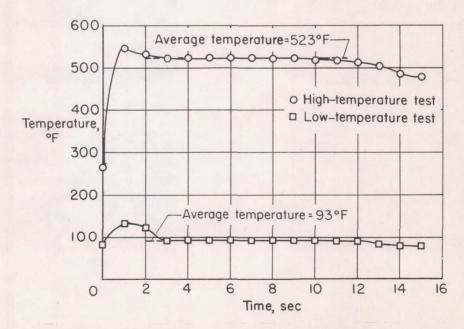
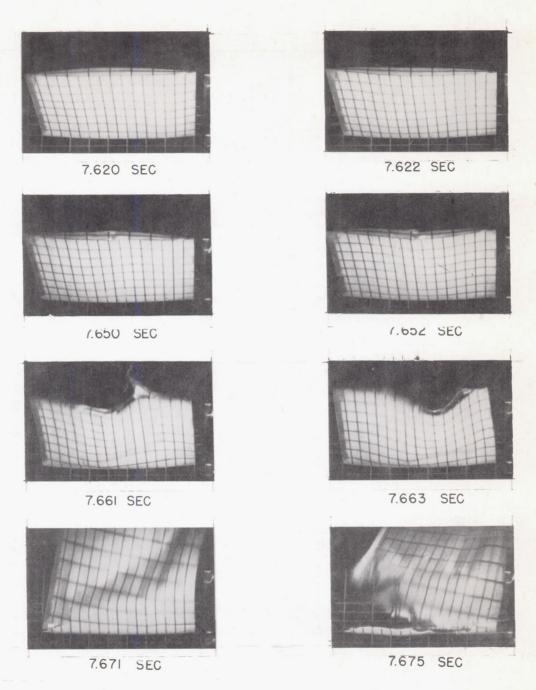


Figure 6.- Typical variation of stagnation temperature with time. Elevated-temperature test data are from test 1 of model MW-18; low-temperature test data are from test 1 of MW-4-(2).



L-57-4443

Figure 7.- Flutter and failure sequence of model MW-4-(2) at $\alpha=0^\circ$. Flutter frequency, 240 cps; air flows from left to right.

37

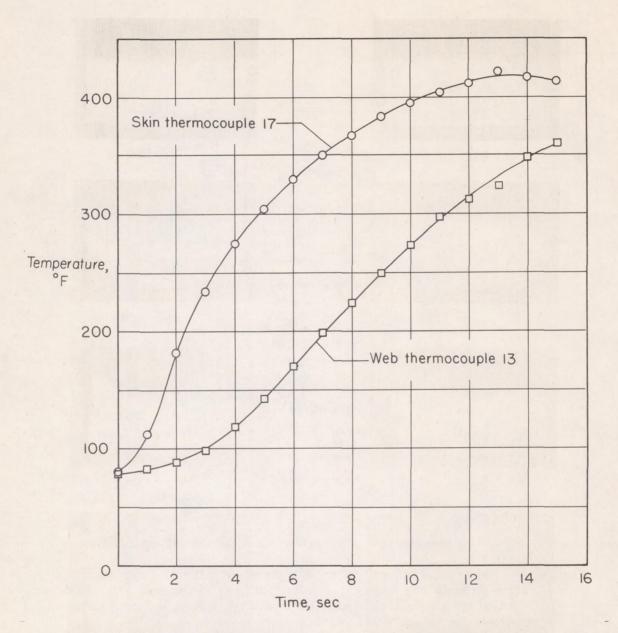
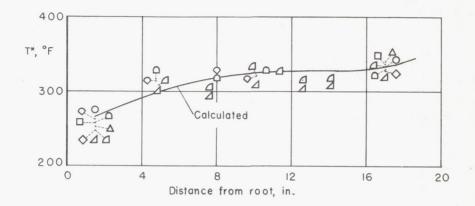


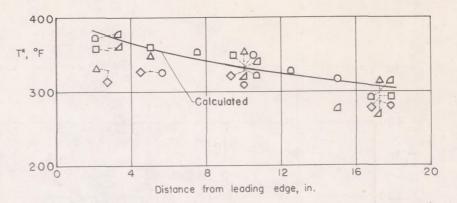
Figure 8.- Typical model temperature histories during a high-stagnation-temperature test. Model MW-18; test 1.



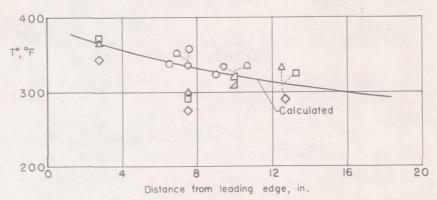
Symbol Model and test

- O MW-4-(2), test no. 2
- ☐ MW-16, test no. 2
- ♦ MW-16, test no. 3
- △ MW-16, test no. 4
- ∠ MW-17, test no.1
- △ MW-17, test no.2
- □ MW-18, test no. I
- Q MW-18, test no.2
- (a) Spanwise temperature distribution along model midchord.

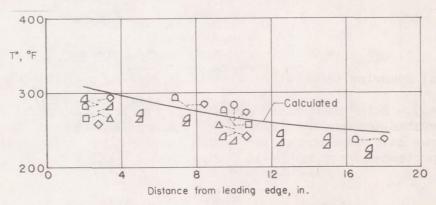
Figure 9.- Skin-temperature distribution at 6 seconds test time for elevated-temperature tests. For comparison purposes, the temperatures have been normalized on the basis of the test conditions experienced by model MW-18 during test 1.



(b) Chordwise temperature distribution at approximately 17.25 inches from the root.

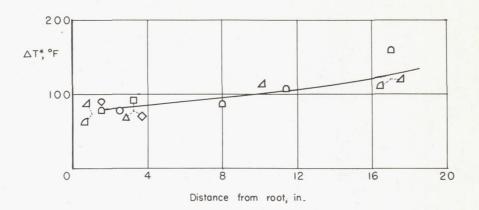


(c) Chordwise temperature distribution at approximately the midspan.

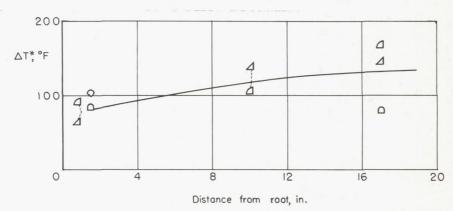


(d) Chordwise temperature distribution at approximately 2 inches from the root.

Figure 9.- Concluded.



(a) Difference in temperature between web 3 and the skin at the midchord.



(b) Difference in temperature between web 4 and the skin at the center chord.

O MW-4-(2), test no. 2 \triangle MW-17, test no. 1 \square MW-16, test no. 2 \triangle MW-16, test no. 3 \square MW-18, test no. 1 \triangle MW-16, test no. 4 \square MW-18, test no. 2

Figure 10.- Difference between skin temperatures and web temperatures at 6 seconds test time.

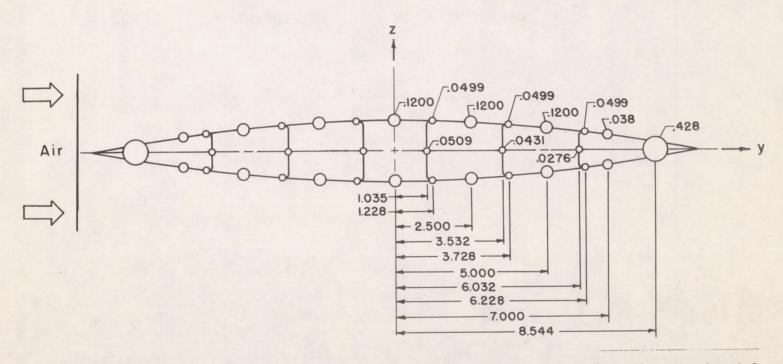


Figure 11.- Idealized cross section used to calculate thermal stresses from the experimental temperature distribution. The cross section is geometrically doubly symmetric.

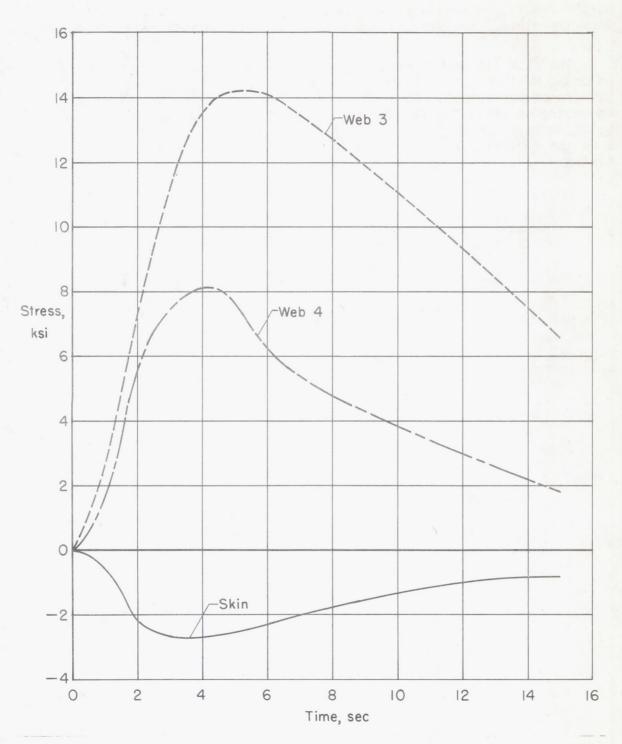


Figure 12.- Calculated stresses about the midchord at a section 3 inches from the tip of model MW-18 during test 1.